CHEMISTRY OF MATERIALS

Article

pubs.acs.org/cm

Oxidation-Induced Trapping of Drugs in Porous Silicon Microparticles

Nicole L. Fry,[†] Gerry R. Boss,[‡] and Michael J. Sailor*,[†]

[†]Department of Chemistry and Biochemistry and [‡]Department of Medicine, University of California at San Diego, La Jolla, California 92093, United States

Supporting Information

ABSTRACT: An approach for the preparation of an oxidized porous silicon microparticle drug delivery system that can provide efficient trapping and sustained release of various drugs is reported. The method uses the contraction of porous silicon's mesopores, which occurs during oxidation of the silicon matrix, to increase the loading and retention of drugs within the particles. First, a porous Si (pSi) film is prepared by electrochemical etching of p-type silicon with a resistivity of >0.65 Ω cm in a 1:1 (v/v) HF/ethanol electrolyte solution. Under these conditions, the pore walls are sufficiently thin to allow for complete oxidation of the silicon skeleton under mild conditions. The pSi film is then soaked in an aqueous solution containing the drug (cobinamide or rhodamine B test molecules were used in this study) and sodium nitrite. Oxidation of the porous host by nitrite results in a shrinking of the pore openings, which physically traps the drug in the porous matrix. The film is subsequently fractured by ultrasonication into microparticles. Upon comparison with commonly used oxidizing agents for pSi such as water, peroxide, and dimethyl sulfoxide, nitrite is kinetically and thermodynamically sufficient to oxidize the pore walls of the pSi matrix, precluding reductive (by Si) or oxidative (by nitrite) degradation of the drug payload. The drug loading efficiency is significantly increased (by up to 10-fold), and the release rate is significantly prolonged (by 20-fold) relative to control samples in which the drug is loaded by infiltration of pSi particles postoxidation. We find that it is important that the silicon skeleton be completely oxidized to ensure the drug is not reduced or degraded by contact with elemental silicon during the particle dissolution–drug release phase.

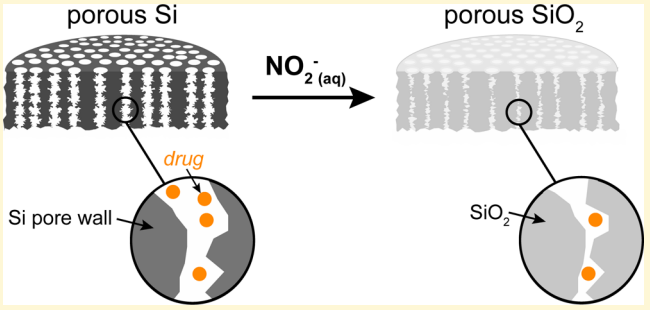

INTRODUCTION

Of the many porous materials being developed for sustained release drug delivery systems,[1−11] electrochemically etched porous silicon (pSi) is an attractive candidate because of its highly tunable nanostructure (micro- to macroporous), chemically modifiable surface,[12] biocompatibility,[13,14] and biodegradability.[15,16] The biodegradation product of pSi is orthosilicic acid [$Si(OH)_4$], which is easily absorbed from the gastrointestinal tract and excreted in the urine.[17,18] It has been shown that pSi nanoparticles loaded with drugs can be injected intravenously and are degraded *in vivo* into benign products excreted by the kidneys.[19]

The large surface area of pSi provides a substantial drug loading capacity.[20,21] However, interaction between the porous matrix and the drug must be carefully considered to design an effective delivery system that provides controlled release of the drug in its active form. Loaded molecules will quickly diffuse out of porous materials because of local concentration gradients unless additional interactions between the porous matrix and drug are generated. Freshly prepared pSi contains highly reactive surface Si−H species with underlying elemental silicon, both of which are good reducing agents.[22,23] For example, the reduction potential of pSi is sufficient to reduce, and thereby inactivate, many organic and inorganic drugs such as doxorubicin,[24] daunorubicin,[25] and cisplatin.[26] Thus modification of pSi is needed to both limit redox degradation of drugs and increase the affinity of the drug for the pSi surface. Various electrostatic or hydrophobic interactions,[6,20,27,28] covalent chemistries,[29−33] or pore capping reactions[26,34,35] have been used to create more effective drug delivery systems.

Here we describe a new oxidative pSi trapping method that is versatile and sufficiently mild to be useful with a range of drugs possessing a wide variety of characteristics (organic or inorganic, hydrophilic or hydrophobic, neutral or positively charged, and/or redox-active). The method relies on the dynamic structure of pSi and physical changes that occur during its oxidation. Electrochemically etched pSi readily oxidizes in aqueous solutions,[19,36] which generally results in reduction of the pore volume because of swelling of the pore walls as oxygen is incorporated into the silicon skeleton (Scheme 1). We hypothesized that pore wall swelling could be used to trap a drug within the pSi framework, provided the dimensions of the initial pores, the oxidized pores, and the drug are in a suitable size range. The redox activity of the pSi matrix with the drug candidate is an additional constraint: to prevent the drug from

Received: March 5, 2014
Published: March 20, 2014

   dx.doi.org/10.1021/cm500797b | Chem. Mater. 2014, 26, 2758−2764

Scheme 1. Illustration Showing the Expansion of the Silicon Matrix (top left) as Oxygen Is Incorporated into the Partially Oxidized (top middle) or Fully Oxidized (top right) Porous Silicon Skeleton[a]

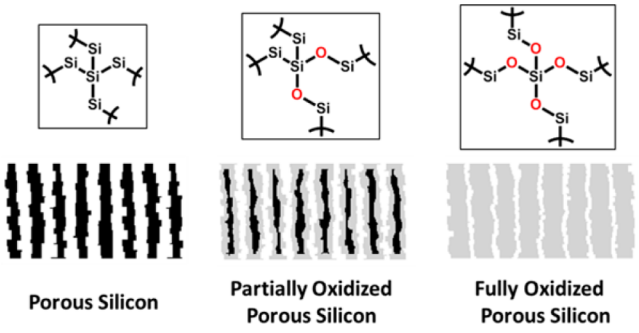

[a]This leads to a decrease in pore diameter as the porous silicon film (bottom left) becomes partially oxidized (bottom middle) and then fully oxidized (bottom left).

being reduced, the silicon skeleton must be oxidized by something other than the drug being trapped. We reasoned that an oxidant of sufficient kinetic and thermodynamic competency and concentration could be preferentially reduced, leaving the trapped drug unaffected. Because water is a relatively weak oxidant, stronger silicon oxidants such as nitrite,[37] peroxide,[38] and dimethyl sulfoxide (DMSO)[39] are candidates, depending on the characteristics of the drug being loaded. Nitrite is an interesting oxidant from the perspective of chemical reactivity. Although it has a good ability to oxidize silicon or Si−H surface bonds, when used as a food preservative it actually suppresses oxidation; in that case, it limits the oxidation of fatty acids by acting as a trap for free radicals derived from oxygen and other reactive oxygen species. This ability of nitrite ion to act as a chemical oxidant for silicon while simultaneously suppressing more deleterious oxidation reactions is a distinctive characteristic of this oxidant in this work.

While we have long suspected that silicon oxidation could be used to load drugs within the pSi framework,[10] we have never specifically tested or validated that this loading technique actually leads to drug trapping and further that the drug is not degraded by the loading process. Thus, in this study, we tested the redox trapping method using cobinamide, a vitamin B_{12} analogue that is being developed as a cyanide antidote.[40−44] We chose cobinamide because its hydrophilicity, small size, and redox-active cobalt center make it difficult to load into porous matrices in its active oxidized state; thus, it presented a greater challenge than most drugs, and if the method worked for cobinamide, it would likely work for other drugs. We compared cobinamide to rhodamine B, a cationic organic dye with limited redox activity, to prove that cobinamide's redox activity was not involved in the oxidation trapping mechanism. The distinctive UV−visible absorbance spectra of cobinamide and rhodamine B provided for quick and easy detection and redox state assessment.

EXPERIMENTAL SECTION

Materials. Boron-doped p-type Si wafers (1−10, 0.01−1, or 0.03−0.05 Ω cm resistivity, ⟨100⟩ orientation) were obtained from International Wafer Service, Inc. Aqueous hydrofluoric acid (48% aqueous), dimethyl sulfoxide, hydrogen peroxide (30% aqueous), hydrochloric acid (1 M), and sodium hydroxide (all ACS grade) were purchased from Fisher Scientific. Absolute ethanol (200 proof) was

Chart 1. Structure of Cobinamide When It is Dissolved in Neutral Aqueous Solutions, with Hydroxide and Water Molecules Bound in the Axial Positions (aquohydroxocobinamide)

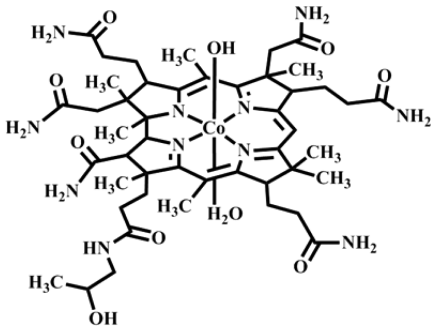

obtained from Rossville Gold Shield Chemicals. Phosphate-buffered saline (1×, pH 7.4) was purchased from Mediatech, Inc. Sodium nitrite and potassium cyanide were obtained from Sigma-Aldrich Chemicals. Pure aquohydroxocobinamide was produced by base hydrolysis of hydroxocobalamin (purchased from Sigma-Aldrich).[49]

Preparation of Porous Silicon Samples. Porous silicon (pSi) films were prepared by anodic electrochemical etching of polished Si wafers. A Teflon etch cell was used that exposed 8 cm^2 of the Si wafer to a 1:1 (v/v) 48% aqueous HF/ethanol mixture. Samples were etched at a constant current density of 32 mA/cm^2 for 1200, 600, and 430 s for samples **1**−**3**, respectively. The pSi films were removed from the crystalline silicon substrate by a current pulse of 5 mA/cm^2 for 50 s in a solution of 3.3% aqueous HF in ethanol. The free-standing pSi films were rinsed with ethanol and dried *in vacuo*.

Preparation of Porous Silicon Microparticles. *Method A: Postoxidation (PostOx).* Dried pSi films (10 mg) were immersed in 1 mL of 25 mM sodium nitrite (pH adjusted to ∼5 with HCl) within a glass vial and fractured into microparticles by ultrasonication for 30 min. The mixture was maintained at room temperature for 24 h to allow further oxidation of the particles, and the particles were washed three times each with water and ethanol by centrifugation and dried *in vacuo* at 60 °C for 2 h. The resulting oxidized particles were added to 1 mL of 5 mM cobinamide or rhodamine B in deionized water (pH adjusted to ∼5 with HCl) and agitated for 16 h at room temperature. The cobinamide- or rhodamine B-loaded particles were then washed three times each with water and ethanol by centrifugation and dried *in vacuo*.

Method B: Oxidation Trapping Loading (OxTrap). A 1 mL solution of 5 mM cobinamide or rhodamine B and 25 mM sodium nitrite in water (pH adjusted to ∼5 with HCl) was added to 10 mg of dried pSi films in a glass vial. The mixture was exposed to ultrasonication for 30 min to fracture the Si films into microparticles and maintained at room temperature for 24 h to allow further oxidation of the particles in the presence of cobinamide or rhodamine B. The particles were washed three times each with water and ethanol by centrifugation and dried *in vacuo* at 60 °C for 2 h.

Physical Characterization of Porous Materials. A scanning electron microscope (FEI XL30) was used to obtain cross-sectional images of the pSi samples. Attenuated total reflectance Fourier transform infrared (ATR-FTIR) spectra were recorded using a Thermo Scientific Nicolet 6700 FTIR instrument with a Smart iTR diamond ATR fixture. Raman spectra were recorded using a Renishaw inVia Raman microscope with a 100 mW, 532 nm laser excitation source. Nitrogen adsorption−desorption isotherms were acquired on the freshly etched materials at 77 K on a Micromeritics ASAP 2020 instrument. Thin film optical interference spectra of the porous Si samples were recorded in a 180° reflection configuration using an unpolarized tungsten light and an Ocean Optics 4000 CCD spectrometer fitted with a bifurcated fiber-optic cable. The optical reflectance spectra were processed using a computer and algorithms described previously.[45]

dx.doi.org/10.1021/cm500797b | *Chem. Mater.* 2014, 26, 2758−2764

Cobinamide and Rhodamine B Release Studies. Porous Si microparticles loaded with cobinamide or rhodamine B were immersed in 1 mL of either deionized water or aqueous phosphate-buffered saline (pH 7.4) at a particle concentration of 100 μg/mL and agitated at room temperature. The supernatant containing released cobinamide or rhodamine B was collected at set times (2, 8, 24, 48, 72, 96, and 120 h) and replaced with fresh water or buffer. Concentrations of released cobinamide were determined by adding excess potassium cyanide to the solution to convert cobinamide to the dicyano form and then measuring the absorbance value at 370 nm (ε = 30000 M^{-1} cm^{-1}). Concentrations of released rhodamine B were determined by the absorbance at 544 nm (ε = 106000 M^{-1} cm^{-1}).

RESULTS AND DISCUSSION

Preparation of a Porous Silicon Matrix. In this study, we were interested in determining how the different porous silicon morphologies generated from silicon wafers with different resistivities (under similar reaction conditions) would affect oxidation of the different silicon structures and how those differences would affect the loading and subsequent release of cobinamide from the silicon matrix. Porous silicon films were prepared from single-crystal silicon ⟨100⟩ wafers with three different resistivities: 1.20, 0.65, and 0.05 Ω cm (samples **1**−**3**, respectively). The silicon wafers were subjected to anodic electrochemical etching in a 1:1 (v/v) aqueous 48% hydrofluoric acid/ethanol electrolyte solution. A constant current density of 32 mA/cm^2 was used to prepare all three samples, but the etch time was varied so that the thickness of each pSi sample was ∼10 μm. We used the spectroscopic liquid infiltration method (SLIM)[45] to determine the thickness and total open porosity of the etched films and found average open porosities of 60% for samples **1** and **2** and 40% for sample **3**. These measurements were confirmed by cross-sectional scanning electron microscopy (Figure S1 of the Supporting Information) and gravimetric analysis. The nanostructure of the pores was characterized using nitrogen adsorption−desorption analysis, with the resulting isotherms exhibiting type IV hysteresis loops, typical of mesoporous materials (Figure 1). Porous silicon films were prepared with different pore morphologies to systematically study the influence of pore size on loading and subsequent release of cobinamide from the silicon matrix. The measured Brunauer−Emmett−Teller (BET)[46] surface areas of the samples were 548, 482, and 299 m^2/g for samples **1**−**3**, respectively. As expected, the pore size increased as the concentration of boron dopant increased for samples **1**−**3** as determined by the mean Barrett−Joyner−Halenda (BJH)[47] pore diameters of 3.6, 4.7, and 5.6 nm, respectively.

Optimization of Silicon Oxidation and Drug Trapping Conditions. The surface chemistry of pSi plays a large role in the adsorption of drugs within the porous matrix. Therefore, we first studied the interaction between cobinamide and the pSi surface of samples **1**−**3** using Fourier transform infrared (FTIR) spectroscopy (Figure 2 and Figures S2 and S3 of the Supporting Information). The presence of silicon hydride species on the surface of freshly prepared pSi was confirmed by FTIR signals assigned to Si−H vibrations, at 2108 and 2084 cm^{-1} (νSiH_2 and νSiH stretching modes, respectively). To study the initial reaction of cobinamide with the surface of the silicon matrix, FTIR spectra of the pSi samples were monitored after exposure to aqueous solutions (pH adjusted to 5 with HCl) with and without cobinamide for 2 h. The FTIR spectrum of the cobinamide-exposed sample (Figure 2C) has an amide stretching frequency at 1660 cm^{-1}, which is characteristic of free cobinamide [FTIR of free cobinamide (Figure S4 of the Supporting Information)] and absent in a control sample exposed to deionized water (Figure 2B). Because the samples were thoroughly washed and dried before FTIR analysis, the presence of the cobinamide peaks in the

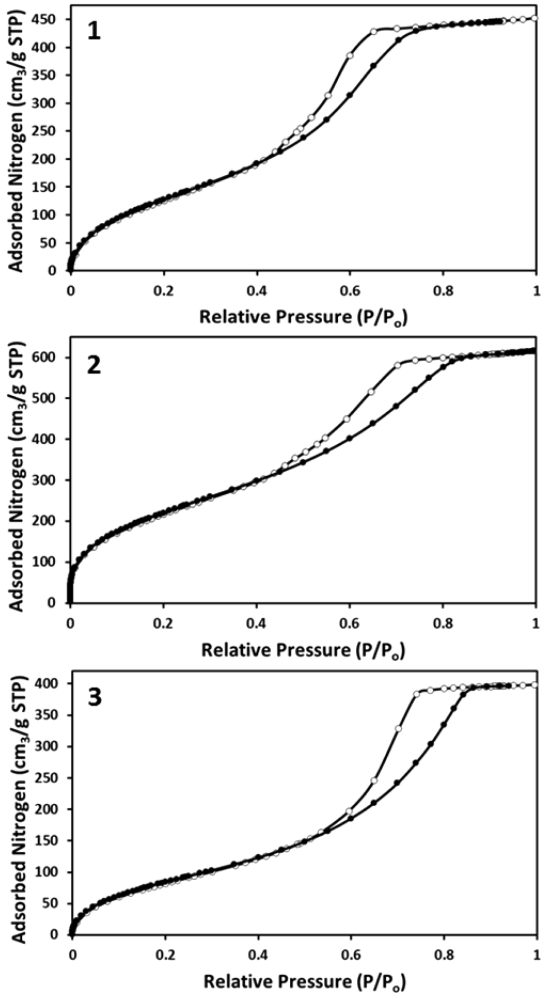

Figure 1. Nitrogen adsorption−desorption isotherms for porous silicon particles prepared from p-type silicon wafers with resistivities of 1.20, 0.65, and 0.05 Ω cm for **1**−**3**, respectively. The adsorption and desorption branches of the isotherms are shown as filled and empty circles, respectively.

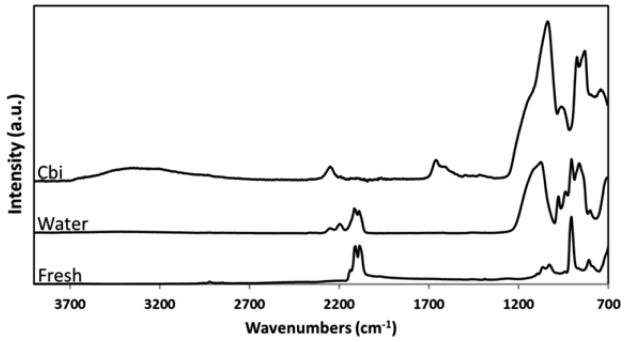

Figure 2. Fourier transform infrared (FTIR) spectra of a freshly etched porous silicon sample of **2** (bottom), **2** exposed to water (middle), or an aqueous cobinamide solution (top) for 2 h. The baselines of the middle and top spectra are offset from the *x*-axis for comparison.

dx.doi.org/10.1021/cm500797b | Chem. Mater. 2014, 26, 2758−2764

spectrum confirms loading of cobinamide in all three pSi samples (**1**−**3**). A broad silicon oxide band (∼1100 cm^{-1}), along with peaks assigned to OxSi-Hy species (2200−2250 cm^{-1}), was also present in both the water- and cobinamide-treated samples. The height of the silicon oxide band compared to those of the OxSi-Hy bands was larger in the cobinamide-exposed sample than in the water-exposed sample. In addition, the magnitudes of the Si−H vibrational bands decreased only slightly for the sample exposed to water alone, while the cobinamide-exposed sample displayed a complete loss of the Si−H signal. These findings suggest that the rate of silicon oxidation was increased in the presence of cobinamide.

The redox interaction between cobinamide and the silicon matrix was investigated further using visible reflectance and absorbance spectroscopy. The optical reflectance spectrum of pSi was used to monitor the rate of silicon oxidation in the presence of cobinamide, while the absorbance spectrum of cobinamide was used to determine whether any redox degradation of cobinamide had occurred. First, silicon oxidation was analyzed by monitoring changes in the optical reflectance spectrum over time of pSi sample **2** exposed to cobinamide. The Fourier transform of these reflectance spectra gave values of $2nL$, or an effective optical thickness of the pSi film.[45] A value of $2nL$ can be used to assess how the refractive index (n) of the material changes over time [assuming any changes in sample thickness (L) are negligible]. Exposing pSi to aqueous cobinamide caused a steady decrease in the value of $2nL$ over time, which can be attributed to a decrease in the refractive index of the sample due to the conversion of Si (nD = 3.8) to SiO_2 (nD = 1.54) (Figure 3). The absorbance spectrum of the

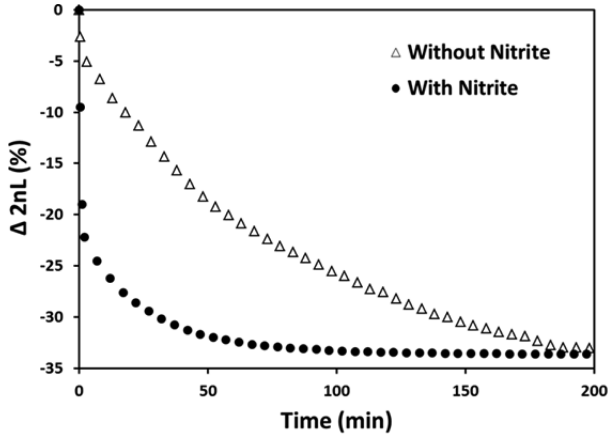

Figure 3. Experimental optical response vs time showing the oxidation of pSi sample **2** upon exposure to aqueous cobinamide solutions with (●) or without (△) nitrite present. The effective optical thickness ($2nL$, where n is the average refractive index and L is the total thickness of the sample) was obtained from the fast Fourier transform of the optical reflectance spectra of both samples obtained at each time point. The quantity $\Delta 2nL$ (%) is defined as $(2nL - 2nL_0)/2nL_0 \times 100\%$, where $2nL_0$ is the value of $2nL$ measured immediately after introduction of the solutions.

cobinamide solution after it had been exposed to pSi for 2 h revealed significant changes compared to that of the original cobinamide solution (Figure 4A). The cobalt center of cobinamide was in the Co^{3+} oxidation state initially; however, the appearance of new absorption peaks at 315 and 470 nm suggested the Co^{3+} center was reduced to Co^{2+} by the pSi. The absorbance of the cobinamide supernatant obtained after the

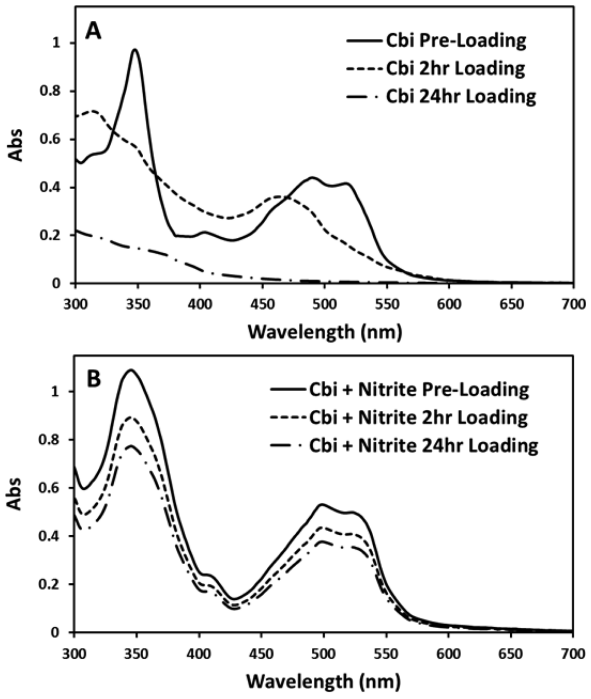

Figure 4. UV−visible absorbance spectra of cobinamide solutions without (A) or with (B) added nitrite. Absorbance spectra of solutions were recorded before they were exposed to pSi particles (—), and absorbance spectra of the supernatants were recorded after periods of pSi particle exposure of 2 (---) or 24 h (−·−).

sample had been exposed to pSi for 24 h revealed a complete loss of the lowest-energy absorption band leaving only a weak, ill-defined absorption spectrum at wavelengths of <400 nm. Such changes suggest substantial alterations, if not complete loss of the cobalt−corrin ring coordination.

To protect the loaded cobinamide from redox degradation, the effect of added oxidants peroxide, nitrite, and DMSO was evaluated. In these experiments, the oxidant was introduced into the cobinamide solution prior to the addition of the pSi sample, so both cobinamide and the oxidant were present in the solution during drug loading. We found that cobinamide was unstable in the peroxide and DMSO solutions but was stable in nitrous acid generated from an acidic sodium nitrite solution [25 mM $NaNO_2$ (pH 5)] (eq 1).

$$4HNO_2 + Si \rightarrow SiO_2 + 4NO + 2H_2O \quad (1)$$

The shift in the $2nL$ value measured for pSi samples exposed to cobinamide dissolved in the acidic nitrite solution decreased much more rapidly compared to the shift in $2nL$ observed upon exposure to cobinamide without nitrite present.

In addition, when cobinamide was loaded into the acidic nitrite solution, no change occurred in the relative height or shape of the peaks observed in the solution absorbance spectrum of cobinamide after exposure to pSi for 2 or 24 h (Figure 4B). Instead, only the overall intensity of the spectrum decreased because of the decreased concentration of free cobinamide in solution, as it became trapped within the pSi matrix. The reflectance and absorbance data both suggest that pSi preferentially reduced the nitrite, thus protecting cobinamide from redox degradation.

To confirm that cobinamide trapped within the pSi matrix was indeed protected by the acidic nitrite solution, loaded samples were exposed to sodium hydroxide (pH 9) to dissolve

dx.doi.org/10.1021/cm500797b | Chem. Mater. 2014, 26, 2758−2764

the porous matrix and release the trapped cobinamide. The absorbance spectra of the released cobinamide loaded in samples **1** and **2** were unchanged compared to the spectrum of preloaded cobinamide, whereas the absorbance spectrum of sample **3** showed signs of redox degradation of the released cobinamide.

Therefore, Raman spectroscopy was used to elucidate the difference in cobinamide protection between silicon sample **3** (derived from the more highly doped p-type Si) and samples **1** and **2**. The Raman spectra of samples **1** and **2** contained peaks identical to those in the spectrum of unloaded cobinamide, with no evidence of elemental (i.e., unoxidized) silicon, whereas the spectrum of sample **3** had an additional peak at 520 cm^{-1} assigned to the Si−Si optical phonon mode of crystalline silicon (Figure 5).[48] Thus, while the silicon matrices of samples **1** and **2** became fully oxidized, some unoxidized silicon remained after the oxidation trapping of cobinamide in sample **3**. This is attributed to the thicker silicon pore walls in sample **3**. Once a certain thickness of silicon oxide had formed on the pore surface, the room-temperature oxidation process was expected to slow considerably. Thus, the pore walls of samples **1** and **2** were sufficiently thin to allow complete oxidation of the Si skeleton. The unoxidized silicon remaining in sample **3** after oxidative loading most likely became exposed during the dissolution of the pSi matrix. This exposed elemental silicon was then able to interact with loaded cobinamide, resulting in the reductive degradation of the drug.

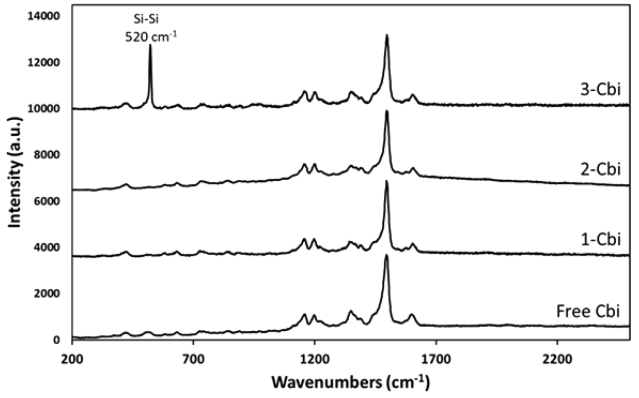

Figure 5. Raman spectra of preloaded cobinamide (Free Cbi) and cobinamide-loaded pSi particles prepared from p-type silicon wafers with resistivities of 1.20 (**1**-Cbi), 0.65 (**2**-Cbi), and 0.05 (**3**-Cbi) Ω cm via oxidative trapping of cobinamide with aqueous nitrite solutions (OxTrap).

Comparison of Oxidative Trapping and Postoxidation Cobinamide Loading Methods. Two different loading methods were compared to determine which provided a higher loading efficiency and more sustained release of cobinamide. For these studies, acidic nitrite solutions were used with pSi samples **1** and **2** to avoid the redox degradation of cobinamide associated with sample **3**. For the oxidative trapping method (OxTrap), cobinamide was dissolved in an acidic nitrite solution, and the solution was added to freshly etched pSi films; the mixture was ultrasonicated for 30 min to form microparticles and maintained at room temperature for 24 h to complete the oxidation process. For the postoxidation loading method (PostOx), the pSi films were also maintained in the presence of the nitrite oxidizing agent during the 30 min ultrasonication and 24 h oxidation periods, but cobinamide was added to the particles after the 24 h oxidation step. Optical microscope images of the loaded microparticles (Figure 6) revealed that the average size of the microparticles was very similar for the two types of PostOx samples studied (21 ± 5 μm for **1** and 22 ± 6 μm for **2**).

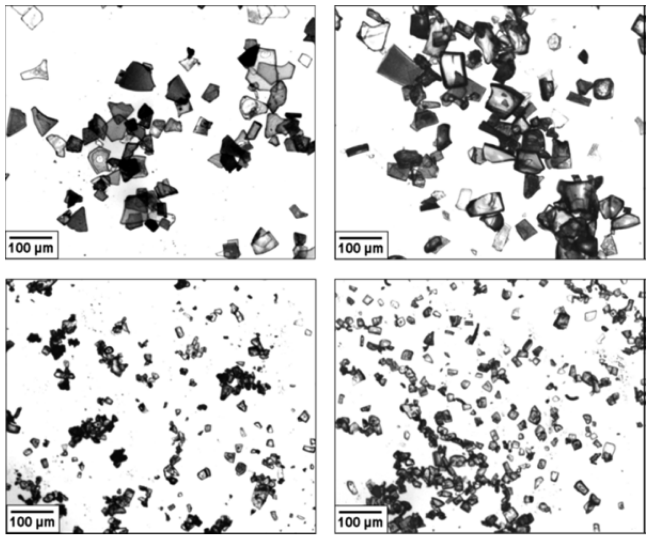

Figure 6. Bright field optical microscope images of microparticles prepared via the oxidation trapping (OxTrap, top) and postoxidation (PostOx, bottom) methods of loading cobinamide. The pSi microparticles were prepared via a 30 min ultrasonication of pSi films of sample type **1** (left) and **2** (right).

Likewise, ultrasonication of either sample **1** or **2** subjected to the OxTrap method yielded particles with similar sizes (46 ± 14 μm for **1** and 48 ± 14 μm for **2**). However, the particles prepared using OxTrap were significantly larger than those prepared using PostOx for both **1** and **2**. Presumably, the simultaneous cobinamide loading and matrix oxidation that occur with the OxTrap method generate a stronger, composite particle that is not as easily fractured by ultrasound energy.

The cobinamide loading efficiency was measured by extracting the loaded cobinamide from the porous Si microparticle matrix via treatment with a sodium hydroxide solution (pH 9). The basic solution dissolved the Si and SiO_2 components of the microparticle, releasing the drug payload into solution. We quantified the cobinamide by converting it into the dicyano form (by adding excess potassium cyanide) and measuring the optical absorbance at 370 nm (ε = 30000 M^{-1} cm^{-1}). The average cobinamide loadings were 20 ± 8 and 86 ± 10 μg of cobinamide/mg of Si for sample **1** and 74 ± 6 and 112 ± 6 μg of cobinamide/mg of Si for sample **2** for the PostOx and OxTrap particles, respectively. Thus, for both samples **1** and **2**, the OxTrap method yielded greater cobinamide loading than the PostOx method, with sample type **2** showing the largest relative increase (1.5−4-fold increased mass loading of drug, relative to that of the PostOx method). The increased cobinamide loading seen with the microparticles of sample **2** is attributed to the pore size (4.7 nm) being larger than that of sample **1** (3.6 nm). The reduction in the average pore size upon oxidation of the silicon matrix is expected to show a more pronounced effect on the efficiency of drug loading as the pore size approaches the diameter of the drug payload, and this is observed in the data. When introduced before oxidation in the OxTrap method, cobinamide can more

freely penetrate the pores, and the silicon oxide can then grow around the cobinamide molecules.

We next tested the retention of cobinamide within the oxidized silicon matrix for the different microparticle formulations. In pure water, the rate of silicon dissolution is relatively slow, which is expected to delay the release of cobinamide trapped within the silicon oxide matrix. If cobinamide is not physically trapped, it will be free to diffuse out of the pores even if the silicon matrix has not degraded. Consistent with these arguments, the release of cobinamide from the PostOx particles was significantly more rapid than from the OxTrap particles for both sample types **1** and **2** (Figure 7A), with 50% of the loaded drug released within 3 h

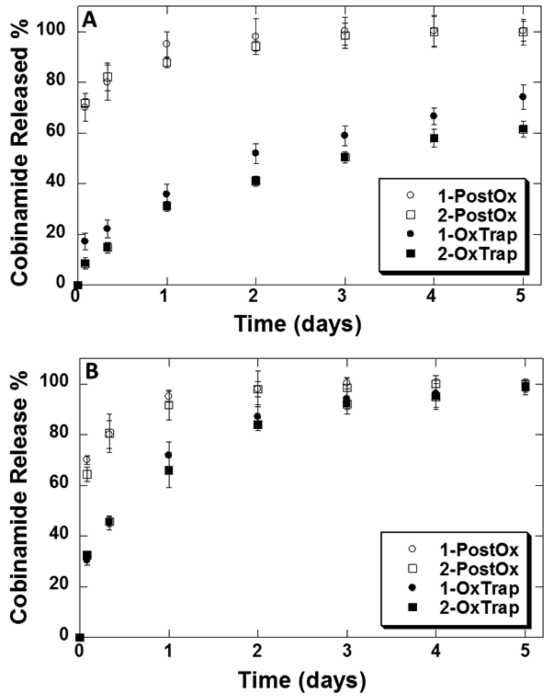

Figure 7. Release of cobinamide into water (A) or aqueous phosphate-buffered saline (B) from oxidized pSi particles **1** (circles) and **2** (squares) loaded with cobinamide via the postoxidation (PostOx, empty symbols) or oxidation trapping (OxTrap, filled symbols) method. The data were averaged from three samples, and the error bars indicate the standard deviation.

for PostOx versus 3 days for OxTrap formulations. This confirms that oxidation of the pSi skeleton in the presence of cobinamide will effectively trap the drug in the pores and that this process increases the level of retention of cobinamide in the resulting microparticles. We observed no significant difference in the cobinamide release rate between samples **1** and **2** for the PostOx-loaded samples and only a slight difference for the OxTrap particles. The slight reduction in the release rate for sample **2** could be due to the slightly larger amount of cobinamide loaded in the particles, which may act to shield the silicon matrix from water dissolution.

The release of cobinamide from the microparticles was also tested in phosphate-buffered saline (PBS), a more physiologically relevant solution (Figure 7B). The pSi matrix degraded more quickly in PBS than in water, although as with pure water, the release profile showed a smaller rate of cobinamide release for the OxTrap than for the PostOx microparticles for both samples **1** and **2**. However, the difference in release rates was less pronounced for the PBS experiments than for the water experiments because of the increased rate of dissolution of silicon in PBS. In addition, for a given preparation (OxTrap or PostOx), we observed no significant difference between the release profiles of sample types **1** and **2**.

To determine if the oxidation trapping method could be used for molecules other than cobinamide, we repeated the loading and release studies of sample type **2** using rhodamine B. We loaded rhodamine B like cobinamide using both the PostOx and OxTrap methods. As for cobinamide, a larger mass loading was achieved with the OxTrap protocol (87 ± 5 μg of rhodamine B/mg of Si) than with the PostOx method (7 ± 1 μg of rhodamine B/mg of Si). The release profiles (in deionized water) for the delivery of rhodamine B from PostOx particles showed more sustained release than from PostOx particles (Figure 8). The data confirmed that the OxTrap method is not specific to cobinamide, providing larger mass loading and more effective trapping for both types of molecules.

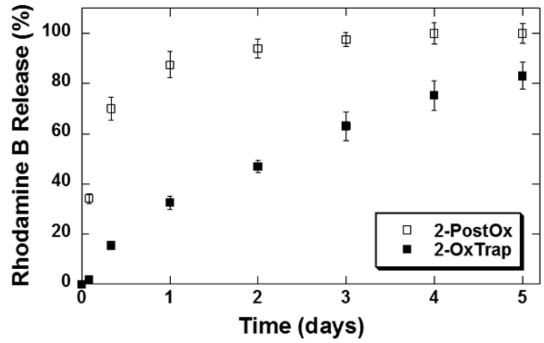

Figure 8. Release of rhodamine B into water from type **2** oxidized porous silicon particles loaded with rhodamine B via the postoxidation [PostOx (□)] or oxidation trapping [OxTrap (■)] method. The data are the means of three samples, and the error bars indicate the standard deviation.

■ CONCLUSIONS

This study focused on the ability of porous Si to shrink its pore dimensions upon mild oxidation of the porous skeleton, to enhance the loading capacity and extend the duration of release of small hydrophilic drugs. Via oxidation of the silicon matrix in the presence of the molecular payload (OxTrap), the molecule was more effectively trapped than it was after simple diffusional loading into a preformed oxide matrix. It was found that the pore and molecule size is a critical parameter in this process; the pore and molecule must be appropriately matched to allow the molecule to diffuse into the unoxidized pore and not diffuse out of the oxidized pore. For cobinamide, the optimal unoxidized pore diameter was between 3.6 and 4.7 nm. For redox-active drugs, the pore wall thickness is an additional important factor. We found that material with smaller pore diameters (and thus thinner pore walls) could be completely oxidized to SiO_2 under mild (room temperature, aqueous nitrite) conditions, whereas material with thicker pore walls retained elemental silicon within the porous skeleton. This residual silicon then reacted with and degraded the cobinamide model drug under long-term aqueous release conditions. In addition, we showed that aqueous acidic nitrite (NO^{2-}) acts as a mild oxidant that does not degrade the model drugs but is sufficiently reactive to oxidize the Si skeleton, outcompeting the reduction of cobinamide by Si and thus preserving the activity

dx.doi.org/10.1021/cm500797b | Chem. Mater. 2014, 26, 2758−2764

of the molecule. We found that porous Si samples prepared in a 1:1 (v/v) HF/ethanol solution from p-type silicon wafers with a resistivity of ∼0.65 Ω cm possess pore walls sufficiently thin to become fully oxidized, whereas the pore walls in porous Si made from silicon with a resistivity of <0.5 Ω cm are too thick and do not become fully oxidized under the OxTrap reaction conditions. This approach may be generally applicable to a wider range of drugs, including more sensitive protein and oligonucleotide therapeutics.

■ ASSOCIATED CONTENT

Supporting Information

Cross-sectional scanning electron microscope images of freshly etched porous Si films **1**−**3** and Fourier transform infrared spectra of **1**, **3**, and free cobinamide. This material is available free of charge via the Internet at http://pubs.acs.org.

■ AUTHOR INFORMATION

Corresponding Author

*E-mail: msailor@ucsd.edu.

Notes

The authors declare no competing financial interest.

■ ACKNOWLEDGMENTS

This material is based upon work supported in part by National Institutes of Health Grants U01 NS058030 and R24 EY022025-01 and National Science Foundation Grant DMR-1210417. We thank Dr. Ronald E. Betts and Douglas Savage for helpful discussions.

■ REFERENCES

(1) Leoni, L.; Desai, T. A. *Adv. Drug Delivery Rev.* **2004**, *56*, 211.
(2) Angelos, S.; Liong, M.; Choi, E.; Zink, J. I. *Chem. Eng. J.* **2008**, *137*, 4.
(3) Horcajada, P.; Chalati, T.; Serre, C.; Gillet, B.; Sebrie, C.; Baati, T.; Eubank, J. F.; Heurtaux, D.; Clayette, P.; Kreuz, C.; Chang, J. S.; Hwang, Y. K.; Marsaud, V.; Bories, P. N.; Cynober, L.; Gil, S.; Ferey, G.; Couvreur, P.; Gref, R. *Nat. Mater.* **2010**, *9*, 172.
(4) Wang, S. B. *Microporous Mesoporous Mater.* **2009**, *117*, 1.
(5) Ferey, G. *Chem. Soc. Rev.* **2008**, *37*, 191.
(6) Gu, L.; Ruff, L. E.; Qin, Z.; Corr, M.; Hedrick, S. M.; Sailor, M. J. *Adv. Mater.* **2012**, *24*, 3981.
(7) Sailor, M. J.; Park, J. H. *Adv. Mater.* **2012**, *24*, 3779.
(8) Xiao, L.; Gu, L.; Howell, S. B.; Sailor, M. J. *ACS Nano* **2011**, *5*, 3651.
(9) Lockwood, R.; McFarlane, S.; Nunez, J. R. R.; Wang, X. Y.; Veinot, J. G. C.; Meldrum, A. *J. Lumin.* **2011**, *131*, 1530.
(10) Anglin, E. J.; Cheng, L.; Freeman, W. R.; Sailor, M. J. *Adv. Drug Delivery Rev.* **2008**, *60*, 1266.
(11) Salonen, J.; Kaukonen, A. M.; Hirvonen, J.; Lehto, V. P. *J. Pharm. Sci.* **2008**, *97*, 632.
(12) Buriak, J. M. *Chem. Rev.* **2002**, *102*, 1272.
(13) Bayliss, S. C.; Buckberry, L. D.; Harris, P. J.; Tobin, M. *J. Porous Mater.* **2000**, *7*, 191.
(14) Low, S. P.; Voelcker, N. H.; Canham, L. T.; Williams, K. A. *Biomaterials* **2009**, *30*, 2873.
(15) Canham, L. T. *Adv. Mater.* **1995**, *7*, 1033.
(16) Anderson, S. H. C.; Elliott, H.; Wallis, D. J.; Canham, L. T.; Powell, J. J. *Phys. Status Solidi A* **2003**, *197*, 331.
(17) Jugdaohsingh, R. *J. Nutr., Health Aging* **2007**, *11*, 99.
(18) Ferrati, S.; Mack, A.; Chiappini, C.; Liu, X. W.; Bean, A. J.; Ferrari, M.; Serda, R. E. *Nanoscale* **2010**, *2*, 1512.
(19) Park, J.-H.; Gu, L.; Maltzahn, G. v.; Ruoslahti, E.; Bhatia, S. N.; Sailor, M. J. *Nat. Mater.* **2009**, *8*, 331.
(20) Salonen, J.; Laitinen, L.; Kaukonen, A. M.; Tuura, J.; Bjorkqvist, M.; Heikkila, T.; Vaha-Heikkila, K.; Hirvonen, J.; Lehto, V. P. *J. Controlled Release* **2005**, *108*, 362.
(21) Zhang, X. G. *J. Electrochem. Soc.* **2004**, *151*, C69.
(22) Laaksonen, T.; Santos, H.; Vihola, H.; Salonen, J.; Riikonen, J.; Heikkila, T.; Peltonen, L.; Kumar, N.; Murzin, D. Y.; Lehto, V.-P.; Hirvonen, J. *Chem. Res. Toxicol.* **2007**, *20*, 1913.
(23) Harper, T. F.; Sailor, M. J. *J. Am. Chem. Soc.* **1997**, *119*, 6943.
(24) Chhablani, J.; Nieto, A.; Hou, H. Y.; Wu, E. C.; Freeman, W. R.; Sailor, M. J.; Cheng, L. Y. *Invest. Ophthalmol. Visual Sci.* **2013**, *54*, 1268.
(25) Wu, E. C.; Andrew, J. S.; Buyanin, A.; Kinsella, J. M.; Sailor, M. J. *Chem. Commun.* **2011**, *47*, 5699.
(26) Park, J. S.; Kinsella, J. M.; Jandial, D. D.; Howell, S. B.; Sailor, M. J. *Small* **2011**, *7*, 2061.
(27) Foraker, A. B.; Walczak, R. J.; Cohen, M. H.; Boiarski, T. A.; Grove, C. F.; Swaan, P. W. *Pharm. Res.* **2003**, *20*, 110.
(28) Anglin, E. J.; Schwartz, M. P.; Ng, V. P.; Perelman, L. A.; Sailor, M. J. *Langmuir* **2004**, *20*, 11264.
(29) McInnes, S. J. P.; Thissen, H.; Choudhury, N. R.; Voelcker, N. H. *J. Colloid Interface Sci.* **2009**, *332*, 336.
(30) Tang, L.; Saharay, A.; Fleischer, W.; Hartman, P. S.; Loni, A.; Canham, L. T.; Coffer, J. L. *Silicon* **2013**, *5*, 213.
(31) Canham, L. T.; Reeves, C. L.; Newey, J. P.; Houlton, M. R.; Cox, T. I.; Buriak, J. M.; Stewart, M. P. *Adv. Mater.* **1999**, *11*, 1505.
(32) Wu, E. C.; Park, J.-H.; Park, J.; Segal, E.; Cunin, F.; Sailor, M. J. *ACS Nano* **2008**, *2*, 2401.
(33) Hartmann, K. I.; Nieto, A.; Wu, E. C.; Freeman, W. R.; Kim, J. S.; Chhablani, J.; Sailor, M. J.; Cheng, L. Y. *J. Ocul. Pharmacol. Ther.* **2013**, *29*, 493.
(34) Perelman, L. A.; Pacholski, C.; Li, Y. Y.; VanNieuwenzhe, M. S.; Sailor, M. J. *Nanomedicine* **2008**, *3*, 31.
(35) Wu, J.; Sailor, M. J. *Adv. Funct. Mater.* **2009**, *19*, 733.
(36) Froner, E.; Adamo, R.; Gaburro, Z.; Margesin, B.; Pavesi, L.; Rigo, A.; Scarpa, M. *J. Nanopart. Res.* **2006**, *8*, 1071.
(37) Steinert, M.; Acker, J.; Henssge, A.; Wetzig, K. *J. Electrochem. Soc.* **2005**, *152*, C843.
(38) Caras, C. A.; Reynard, J. M.; Bright, F. V. *Appl. Spectrosc.* **2013**, *67*, 570.
(39) Song, J. H.; Sailor, M. J. *Inorg. Chem.* **1998**, *37*, 3355.
(40) Broderick, K. E.; Potluri, P.; Zhuang, S. H.; Scheffler, I. E.; Sharma, V. S.; Pilz, R. B.; Boss, G. R. *Exp. Biol. Med.* **2006**, *231*, 641.
(41) Broderick, K. E.; Balasubramanian, M.; Chan, A.; Potluri, P.; Feala, J.; Belke, D. D.; McCulloch, A.; Sharma, V. S.; Pilz, R. B.; Bigby, T. D.; Boss, G. R. *Exp. Biol. Med.* **2007**, *232*, 789.
(42) Chan, A.; Mohammad, O.; Blackledge, W.; Balasubramanian, M.; Boss, G. R.; Bigby, T. D. *Am. J. Respir. Crit. Care Med.* **2009**, 179.
(43) Brenner, M.; Kim, J. G.; Lee, J.; Mahon, S. B.; Lemor, D.; Ahdout, R.; Boss, G. R.; Blackledge, W.; Jann, L.; Nagasawa, H. T.; Patterson, S. E. *Toxicol. Appl. Pharmacol.* **2010**, *248*, 269.
(44) Brenner, M.; Kim, J. G.; Mahon, S. B.; Lee, J.; Kreuter, K. A.; Blackledge, W.; Mukai, D.; Patterson, S.; Mohammad, O.; Sharma, V. S.; Boss, G. R. *Annals of Emerging Medicine* **2010**, *55*, 352.
(45) Sailor, M. J. *Porous Silicon in Practice: Preparation, Characterization, and Applications*; Wiley-VCH: Weinheim, Germany, 2012.
(46) Gregg, S. J.; Sing, K. S. W. *Adsorption, Surface Area and Porosity*, 2nd ed.; Academic Press Inc.: London, 1982.
(47) Brunauer, S.; Emmett, P. H.; Teller, E. *J. Am. Chem. Soc.* **1938**, *60*, 309.
(48) DeWolf, I. *Semicond. Sci. Technol.* **1996**, *11*, 139.
(49) Blackledge, W. C.; Blackledge, C. W.; Griesel, A.; Mahon, S. B.; Brenner, M.; Pilz, R. B.; Boss, G. R. *Anal. Chem.* **2010**, *82*, 4216.